NONLINEAR BEAM OPTICS WITH REAL FIELDS IN COMPACT STORAGE RINGS

Herbert O. Moser, Berthold Krevet
Kernforschungszentrum Karlsruhe
Institut für Kernverfahrenstechnik
Postfach 3640
D-7500 Karlsruhe 1, FRG

Alex J. Dragt
Center for Theoretical Physics
Department of Physics and Astronomy
University of Maryland
College Park, Maryland 20742, USA

Abstract: We analyze the proposed Karlsruhe electron storage ring for X-ray in-depth lithography using the 3rd order charged particle beam transport code MARYLIE 3.0. The ring features four 90° superconducting bending magnets. A numerical calculation of their field provides the longitudinal dependence of the multipole expansion coefficients. These are used by the code SCB to compute the Lie algebraic transfer map. Subsequent particle tracking with MARYLIE is employed to find dynamic apertures. Two different magnet designs which both lead to satisfactory dynamic apertures are presented.

Introduction

The worldwide effort to design and construct a compact electron storage ring as source of synchrotron radiation for X-ray lithography has become considerably more intense during the past few years [1-8]. These compact storage rings are characterized by the use of strongly curved large-bore bending magnets which are superconducting in most of the designs. The storage ring proposed at Karlsruhe as a source for X-ray in-depth lithography features a characteristic wavelength of 0.2 nm, an electron energy of 1.4 GeV, a bending radius of 1.2 m obtained with a field of 4 T, and a circumference of 27 m [3,4]. For this kind of bending magnet, the linear isomagnetic treatment of beam optics and particle tracking is no longer adequate. We therefore employ the 3rd order charged particle beam optics and tracking code MARYLIE 3.0 [9]. This enables us to approximate the real fields through 3rd order taking into account their longitudinal dependence along the beam path. An important consequence is that the closed orbit passes through regions where the multipolar field components do not vanish which affects the shape of the dynamic aperture, too. We present two different designs of 90° superconducting bending magnets both leading to useful dynamic apertures when suitably incorporated into the standard lattice of the proposed Karlsruhe lithography ring.

Method

Fig. 1 shows a schematic of the coordinates used. Into a cartesian frame x,z we place a reference trajectory consisting of a leading straight section, a 90° bend, and a trailing straight section. The straight sections enclose an angle of 45° with the x- and z-axis, respectively. Apart from the symmetry to the mid-plane the system is assumed to be symmetric with respect to that plane which is perpendicular to the mid-plane and to the z-axis, and which goes through the center of the circular arc. The magnetic field is calculated using the Biot and Savart law. In the case of the magnet MS6 with its rectangular cross-section an arc routine based on formulae given in ref. [10] is applied. The integration over the arc angle is done in pieces less than 10° wide. In the case of the magnet E24 with its circular cross-section the contribution of the conductors running parallel to the reference orbit is again treated with the arc routine after fitting the coil sectors shown in fig. 2 with arcs. The field of the windings in the end region is

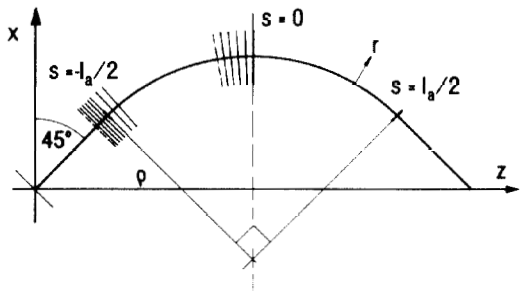

Fig. 1: Geometry used for computing magnetic field in and transfer map of a 90° bending magnet with mid-plane symmetry. Actually, the bending radius ρ is 1.2 m, the length of the leading and trailing straight sections 0.61 m.

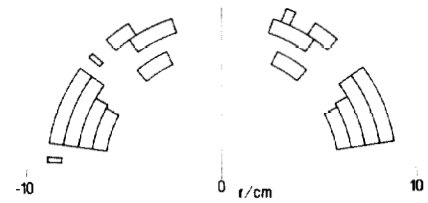

Fig. 2: Cross-section of the upper half of dipole E24. The unsymmetric sectors in the 4th shell reduce the influence of the curvature.

calculated using a filament method. The field is then harmonically analyzed within a number of 36 auxiliary planes which intersect the reference orbit perpendicularly (fig. 1) to find the coefficients of the field expansion in the mid-plane $B(r,s) = b_0(s) + b_1(s)r + b_2(s)r^2/2 + b_3(s)r^3/6$ at different values of s. The s dependence is then fitted by a cubic spline. In this way, the field in the mid-plane and its various derivatives needed can be expressed by analytical formulae and evaluated by inserting the numerically determined expansion coefficients.

In order to be able to make use of the code MARYLIE for beam optics and particle tracking the Lie algebraic transfer map describing a specific magnet must be determined. This is done by the code SCB [4] which solves the equations of motion for the closed orbit (design orbit), the transfer matrix M and the polynomials f_3 and f_4 as defined in [11]. A similar code was written by R. Ryne [12]. SCB contains also routines to compute the values in the mid-plane of the field and its derivatives needed from the expansion coefficients read in from a file written previously by the magnetic field code. A first MARYLIE run is made to bring the map into the form required by MARYLIE (reverse factorization). Then, the lattice can be composed from standard MARYLIE beam line elements plus the map for the bending magnet. We omit a description of the lattice for the sake of brevity and refer the interested reader to ref. [3] and [4].

Results

Magnet designs: Figures 2 and 3 show the cross section and the plan view of the coils projected on the mid-plane, for the case E24. This magnet is based on the Fermilab-HERA design and has 4 shells with the coils distributed such as to minimize the sextupolar and octupolar contributions. At the end of the magnet, the coils are bent up and led to the other side in such a way that the projection onto the mid-plane results in the curves shown in fig. 3. An inconvenience of this design is the unfavourable curvature of the coil at the inner side which makes manufacturing more complicated. However, the two inner shells of E24 are presently fabricated by industry [13] as one double pancake in order to demonstrate the feasibility. No severe problem was encountered, so far. The complication by unfavourable curvature can be avoided by design MS6 (fig. 4). Here, each of the inner windings is individually closed outside so that there is no need to cross the orbit with a coil. In contrast to case E24, this design is not yet optimized with respect to the size of the magnet. Figure 5 displays the total field as well as the sextupole and octupole components versus the position s on the reference orbit for both cases.

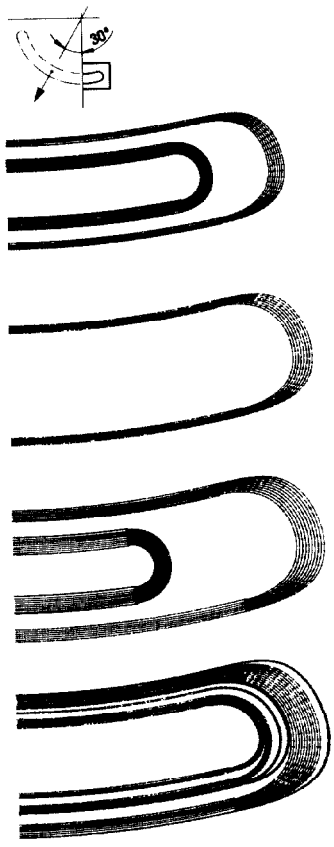

Fig. 3:

Top view of the windings at the end of magnet E24. The four shells are represented separately. Only a region extending from an angle of 30° referred to the 45° symmetry plane up to the end is shown.

Beam optics: Figure 6 shows the difference between the x coordinates of the reference and the design orbit, $\Delta x = x_{ref} - x_{dsg}$, and the field on the design orbit versus the coordinate z for the two magnets E24 and MS6 and for a field described by the formula $B = B_0(1 + \tanh(s/d))/2$ with d = 0.2 m (D20) as defined in [4]. As expected, the design orbit deviates from the reference orbit due to the influence of the field in the end region. In the case E24, the total field reverses its sign in the end region due to the coils crossing the reference orbit, whereas in the cases MS6 and D20 the field drops monotonically keeping its sign. The result is that in case of magnet E24 the deviation of the design from the reference orbit changes sign, too, which results in a much smaller overall deviation than in the cases MS6 and D20.

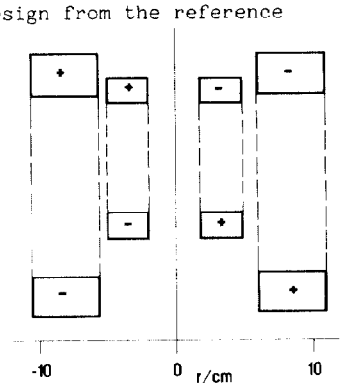

Fig. 4:

Cross-section of the upper half of dipole MS6. The dashed lines indicate the windings at the end which do not cross the electron orbits.

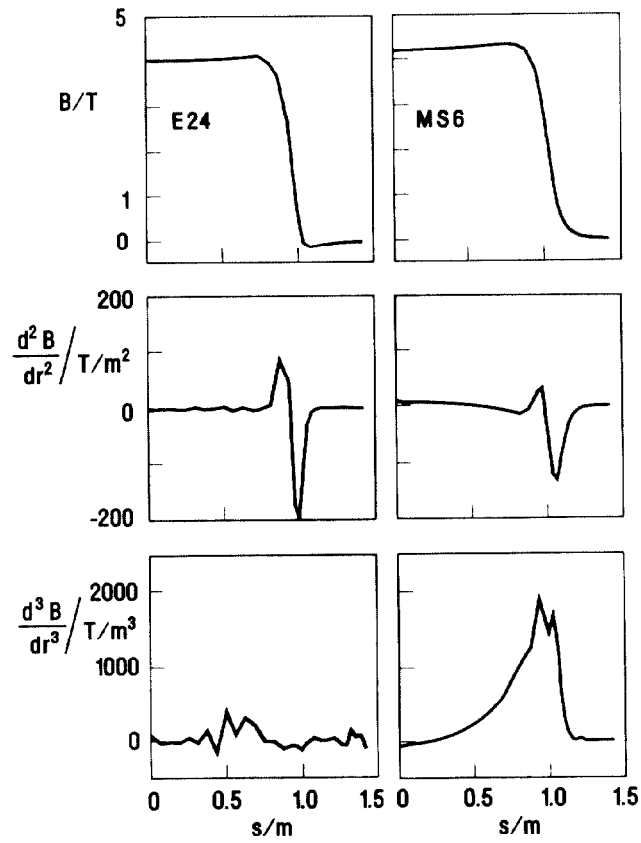

Fig. 5: Total field, sextupole and octupole components of dipoles E24 and MS6 versus path length s along reference orbit.

Figure 7 presents the results of the dynamic aperture calculations. A particle is thrown in with horizontal and vertical deviations x and y from the design orbit, respectively, with zero transverse momenta, and with design momentum, at a location along the design orbit which is situated halfway between bending magnets. Then, the particle is tracked 10^4 times around the ring. For initial conditions lying under the dynamic aperture curves the tracking is stable. Four different curves are displayed. They represent the results obtained when either one of the magnets E24, MS6, D20, or a composition of the MARYLIE beam line elements "normal bend with hard edge fringe fields" preceded and followed by 0.61 m long straight sections are put into the standard lattice.

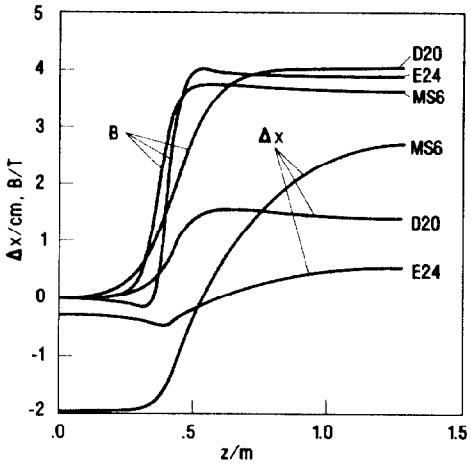

Fig. 6: Deviation of closed orbit (design orbit) from reference orbit, $\Delta x = x_{ref} - x_{dsg}$, and magnetic field on design orbit versus z for the two superconducting magnets MS6 and E24 and for the analytical case D20.

The first remark is that for both magnets, E24 and MS6, the dynamic aperture region is pretty larger than the $10\sigma_x \cdot 10\sigma_y$-rectangle which is favourable for quantum lifetime. Next, the curves are not symmetric with respect to x = 0 mainly due to the asymmetry of the design orbit as shown by the curves for E24, MS6, and D20, but also as a consequence of the asymmetry of an individual trajectory within the bending magnets as suggested by the curve labelled "without end fields". The symmetry with respect to the mid-plane is built in and was checked occasionally. In the cases E24 and MS6, the initial deviation of the design orbit was chosen by a guess aimed at obtaining a minimum overall deviation. This procedure may be optimized in order to achieve maximum dynamic aperture for a given design and lattice. The difference between the curve "without end field" and either one of the cases with end field gives an indication of the relative importance of the nonlinearities coming from the insertion of "real magnets" instead of idealized beam line elements. The magnitude of this effect clearly justifies the nonlinear treatment including "real" fields.

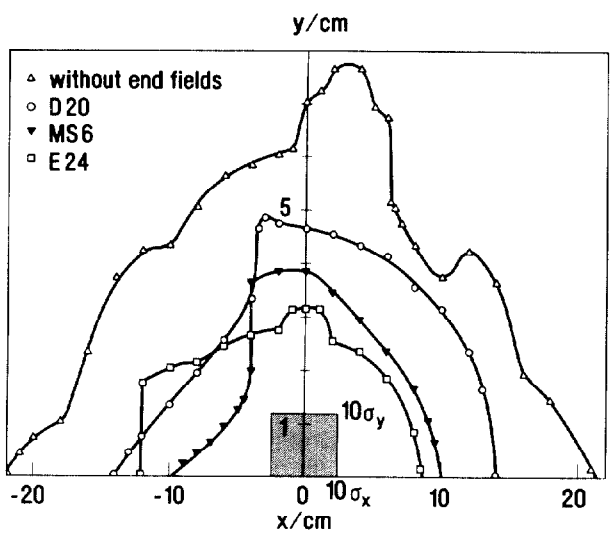

Fig. 7: Dynamic aperture for particles with design momentum in the standard lattice [3,4]. The four curves refer to the different cases of 90° bending magnets used. The rectangle indicates the 10 standard deviation area with full vertical coupling assumed.

References

[1] U. Trinks, F. Nolden, A. Jahnke, "The Table-Top Synchrotron Radiation Source 'Klein-Erna'", Nucl. Instrum. Methods, vol. 200, pp. 475-479, 1982.

[2] E. Weihreter, K. Derikum, H.-H. Flessner, N. Holtkamp, W.-D. Klotz, H. Lehr, R. Maier, M. Martin, L. Schulz, "Injection Studies and Beam Behaviour at Low Energy for the COSY Compact Electron Storage Ring", this conference.

[3] D. Einfeld, O.F. Hagena, P.R.W. Henkes, R. Klingelhöfer, B. Krevet, H.O. Moser, G. Saxon, and G. Stange, "Entwurf einer Synchrotronstrahlungsquelle mit supraleitenden Ablenkmagneten für die Mikrofertigung nach dem LIGA-Verfahren", Report KfK 3976, Kernforschungszentrum Karlsruhe, 1986.

[4] H.O. Moser, A.J. Dragt, "Influence of Strongly Curved Large-Bore Superconducting Bending Magnets on the Optics of Storage Rings", Nucl. Instrum. Methods, to be published, 1987.

[5] Y. Miyahara, K. Takata, T. Nakanishi, "Superconducting Racetrack Electron Storage Ring and Coexistent Injector Microtron for Synchrotron Radiation", Technical Report of ISSP, Ser. B, No. 21, Institute for Solid State Physics, University of Tokyo, 1984.

[6] N. Takahashi, "Compact Superconducting SR Ring for X-Ray Lithography", Nucl. Instrum. Methods, to be published, 1987.

[7] M.Q. Barton, B. Craft, G.P. Williams (eds.), Report of the 2nd Workshop on Synchrotron Radiation Sources for X-Ray Lithography, Brookhaven National Laboratory, BNL 38789, 1986; G.A. Decker, B.C. Craft, "Optimization of Compact Synchrotron Optics for X-Ray Lithography", this conference.

[8] C. Mileikowsky, "The Microtron for X-Ray Lithography", Nucl. Instrum. Methods, to be published, 1987.

[9] A.J. Dragt, R.D. Ryne, L.M. Healy, F. Neri, D.R. Douglas, and E. Forest, "MARYLIE 3.0, A Program for Charged Particle Beam Transport Based on Lie Algebraic Methods", University of Maryland, 1985; A.J. Dragt, "Lectures on Nonlinear Orbit Dynamics", in Physics of High Energy Particle Accelerators, AIP Conf. Proc. No. 87, R.A. Carrigan et al. (eds.), Am. Inst. Phys., New York, 1982.

[10] A. Schleich, A. Segessemann, "Calculation of the Electromagnetic Forces Acting on the Coils of an Electromagnet", in Proc. 3rd Int. Conf. Magnet Technology,edited by Editorial Committee MT3, DESY, Adam Curtze KG, Hamburg, 1971, pp. 198 - 208.

[11] A.J. Dragt, E. Forest, "Computation of Nonlinear Behavior of Hamiltonian Systems Using Lie Algebraic Methods", J. Math. Phys., vol. 24, pp. 2734 - 2744, 1983.

[12] R.D. Ryne, A.J. Dragt, "Numerical Computation of Transfer Maps Using Lie Algebraic Methods", this conference; R.D. Ryne, "Numerical Computation of the Transfer Map for a Magnetic Dipole with Mid-Plane Symmetry Using Lie Algebraic Methods", unpublished, 1986.

[13] Brown, Boveri & Cie, Mannheim, FRG.